

Identification of *Oblique* and *Coplanar Inclined* Fluorescent J-Dimers in Rhodamine 110 Doped Sol-Gel-Glasses

Francisco del Monte and David Levy*,†

Instituto de Ciencia de Materiales de Madrid, CSIC, Cantoblanco, Madrid, 28049 Spain

Received: May 5, 1999; In Final Form: July 7, 1999

Rhodamine 110 (R110) fluorescent J-dimers have been first observed in doped silica gel-glasses made by sol-gel process. The R110 doped gel-glasses photophysical properties such as excitation/fluorescence spectra and lifetimes were studied in a wide range of dye concentrations. It has been determined that the formation of R110 dimers is a consequence of the dye adsorption on the porous surface of the gel-glasses. The adsorption geometry, which is established by the angle formed between the longitudinal axis of the molecule and the gel surface, determined the formation of either R110 fluorescent J-dimers or nonfluorescent H-dimers. Since the adsorption angle was related to the dye concentration, the transition from J-dimers to H-dimers was found for a specific R110 concentration. Formation of J-dimers with a preferential *oblique* or *coplanar inclined* configuration was induced by the change of the polar character of the adsorption surface.

Introduction

Organic dyes have been widely incorporated into gel-glasses prepared by sol-gel^{1,3} in order to use the transparent inorganic matrix as a host for the future applications of the organic molecule.^{4–7} Usually, in the preparation of dye-doped matrixes, the dye concentration is arbitrary selected, even though the concentration may determine the photophysical properties of the system; e.g., high dopant concentration is usually avoided because of the well-known appearance of nonfluorescent dimers, which results in a loss of the fluorescence properties.^{8–11} However, this concentration requirement is ambiguous and should be carefully specified since the formation of fluorescent dimers has recently been reported in Rhodamine B (RB) doped gel-glasses¹² for a certain range of concentrations.

The formation of RB dimers is related to the specific dye adsorption on the porous silica surface. When adsorption takes place, the formation of whether fluorescent or nonfluorescent dimers (J or H, respectively) is related to the molecular adsorption geometry on the surface.^{13,14} This geometry is defined by the angle (ϕ) formed between the longitudinal axis of the molecules (monomer transition moments) and the adsorption surface (Figure 1). Thus, the formation of J-dimers has been reported for ϕ values ranging 0–55° with their respective *oblique* or *coplanar inclined* configurations, while over those angle values H-dimers are formed ($\phi > 55^\circ$, Figure 1).^{15,16} In sol-gel matrixes, the conversion from J-dimers to H-dimers can be achieved because of the relation between the ϕ value and the dye concentration used in the preparation; i.e., since the adsorption surface is fixed, the increase of the number of molecules to be adsorbed implies an increase of the adsorption angle.

In this paper, R110-doped gel-glasses were prepared for a wide range of dye concentrations. The feasibility of R110 to form J-dimers adsorbed on the porous surface was studied by the analysis of the fluorescence properties (both spectral and

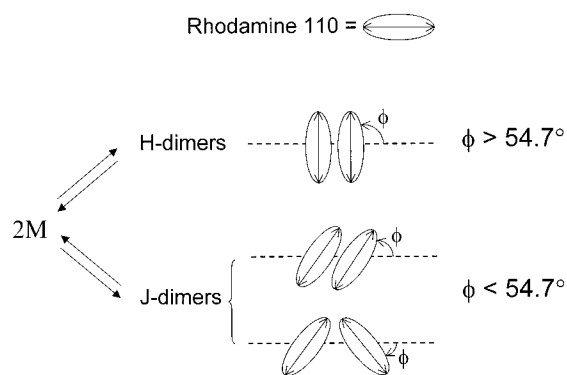


Figure 1. Formation of nonfluorescent H dimers or fluorescent J dimers as a consequence of the geometry adopted by the transition dipoles, from Kemnitz et al.¹³

dynamic properties). Special attention will be focused on the adsorption behavior of R110 as compared to RB. Thus, the similar molecular structures of RB and R110 (groups linked to the nitrogen atom $-NR_2$: $R=H$ for R110 and CH_2-CH_3 for RB)^{17,18} will clarify whether the results observed for RB¹² showed a single case, or they could be extended to other xanthene type molecules.

We also examined the formation of J-dimers at a low R110 concentration through the preparation of gels with different specific surface area available for adsorption. The dimer formation in terms of *oblique* or *coplanar inclined* configurations¹⁹ was also studied.

Experimental Section

Materials. R110 from Aldrich, was used as received without further purification. Tetramethyl orthosilicate (TMOS) from Aldrich, spectrophotometric grade methanol from Merck, and distilled and deionized water (DDW) were also used for sample preparation.

Sample Preparation. Gel-glasses (gels 1–6) were prepared from 9.1 mmol of TMOS, 36.4 mmol of H_2O (water-to-monomer ratio, $r_{w/m} = 4$), and 33 mmol of methanol. A variable

† Instituto Nacional de Tecnología Aeroespacial, INTA, Laboratorio de Instrumentación Espacial-LINES, Torrejón de Ardoz, Madrid, 28850 Spain.

TABLE 1: R110 Moles Used in the Preparation of Gel-Glasses 1–7

	gel 1	gel 2	gel 3	gel 4	gel 5	gel 6	gel 7
moles of R110 $\times 10^7$	0.03	0.075	0.3	1.2	2.4	4.8	0.3

amount of R110 was added to the solution without further prehydrolysis (Table 1). The mixture was allowed to stir during 30 min to get a homogeneous phase. The polymerization was carried out at room temperature in glass bottles covered with aluminum foil. After gelation occurred, the aluminum foil was perforated to allow the slow evaporation of the solvents until the formation of dried xerogels. The samples were kept in the dark along the study.

An additional gel-glass (gel 7) was prepared from 9.1 mmol of TMOS, 9.1 mmol of H₂O ($r_{w/m} = 1$), 33 mmol of methanol, and 3×10^{-8} mmol of R110 (Table 1). The mixture was allowed to stir during 30 min to get a homogeneous phase. The polymerization was carried out at room temperature in glass bottles covered with aluminum foil. After gelation occurred, the aluminum foil was perforated to allow the slow evaporation of the solvents, as well as the adsorption of water from air (room relative humidity ~ 30 – 40%) to exceed the understoichiometric starting conditions, until the formation of the dried xerogel. The sample was kept in the dark along the study.

Preparation of gel 7 in understoichiometric water to monomer molar ratio conditions ($r_{w/m} = 1$) was done in an attempt to reduce the S_A of the porous gel-glass, with no modification of the porous chemical environment (Si–OH groups).²⁰ In other works, the reduction of S_A has been achieved through high-temperature drying processes, promoting the condensation of Si–OH groups placed on the porous surface and the subsequent elimination of water.²¹ However, thermal degradation of organic components avoids these processes for organic-doped gel-glasses. A different alternative for controlling the final properties of the gel-glasses (e.g., porosity) is the modification of the reaction conditions at the sol stage.^{6,22} Use of acid catalyst yield in the formation of very close porous gel-glasses,²³ but acid may also modify the spectroscopic properties of the dye.²⁴ Moreover, the use of drying control chemical additives (DCCA, e.g., surfactants) yield in the formation of controlled porous gel-glasses. However, changes in the dye environment also modify the dye fluorescent properties.²⁵

Instrumentation. The specific surface area (S_A) was measured in an Omnisorp 100 (Coulter) on samples treated under vacuum at 40–60 °C overnight using the BET method (nitrogen gas). The adsorption surface area for gel 7 was around 36 m²/g, while for gels 1–6 adsorption surface area was around 390 m²/g (no modification of S_A was observed for different dye concentrations²⁶).

Infrared Spectroscopy (FT-IR). Infrared spectra were carried out in a Nicolet FT-IR spectrophotometer model 20SXC. Samples were in the form of mixed KBr-gel-glass disks.

Spectroscopy and Lifetimes. Multifrequency modulation, phase analysis, and fluorometric measurements were performed at 25 °C on a 48000s (T-Optics) spectrofluorometer from SLM-Aminco. The instrument is configured for software controlled variable frequency light modulation from 100 Hz to 120 MHz. A front face sample holder for the samples was used for data collection and oriented at 60° in order to minimize light scattering from the excitation beam on the cooled R-928 photomultiplier tube. A D-glycogen scatter solution was used as the reference for lifetime measurements. Appropriate filters were used to eliminate Rayleigh and Raman scatters from the emission. Excitation and emission spectra were corrected for

the wavelength dependence of the 450 W xenon arc excitation but not for the wavelength dependence of the detection system. Spectroscopic and temporal properties were measured by reflection (*front face mode*) on finely ground samples and placed in quartz cells with 1 mm path length. No attempt was made to remove adsorbed or dissolved molecular oxygen from the doped materials. Reference samples that do not contain any fluorescent dopant were used to check the background and optical properties of the gel-glasses.

Phase-resolved fluorescence spectroscopy²⁷ (PRFS) was used for lifetime measurements. The method provides two separated determinations of the fluorescence lifetimes resulting from the phase and modulation, which are independent measurements. Each phase and modulation value is the average of 100–200 readings. The frequency dependent phase and modulation data were analyzed using a nonlinear least-squares procedure that minimizes the squared deviations between the observed and the expected phase and modulation values. The values of the floating parameters (lifetimes and fractional intensities of each fluorophore contributing to the total fluorescence intensity) are varied in a direction that minimizes the value of the deviations between the model and the data χ_R^2 (the reduced error). Computation is finished with a number of iterations through the fitting algorithm, when a minimum is found. The uncertainty in any phase or modulation measurement could be decreased to very small levels averaging in minutes. Specifically, values of χ_R^2 greater than unity may indicate either the presence of systematic errors²⁸ or an inappropriate model. We collected phase and modulation data measured at 20–25 modulation frequencies and additional measurements did not seem to improve the resolution. An uncertainty of 0.5 to the resolution of the phase and 0.005 to the resolution of the modulation was applied for the calculation of χ_R^2 . The accuracy of the lifetime values measured was determined according to the lower χ_R^2 value found in each individual measurement.²⁹

Steady-State Anisotropy. Steady-state anisotropy was measured in *right angle* mode on bulk samples of squared shape with 0.5 cm of path length. Steady-state anisotropy measurements provide insight into the average environment about the fluorescent probe. The fluorescence anisotropy is dependent on the rotational dynamics of the fluorescent probe.³⁰ If a sample is excited by vertically polarized light, its anisotropy $\langle r \rangle$ is given by^{31,32}

$$\langle r \rangle = \frac{I_{||} - I_{\perp}}{I_{||} + 2I_{\perp}} \quad (1)$$

where $I_{||}$ and I_{\perp} are the parallel and the perpendicular components of the total fluorescence, respectively.

Results and Discussion

1. Formation of Fluorescent J-Dimers in R110-Doped Gel-Glasses. The lifetime of the doped silica gel-glass having a low R110 concentration (gel 1, Table 2) was analyzed through the application of PRFS (Figure 2). The analysis let in the determination of a single lifetime for gel 1. Since the number of resolved lifetimes is related to the number of emitting species,^{33,34} a single emitting species must be the responsible of the gel 1 fluorescence emission. Moreover, the value of the gel 1 lifetime was markedly larger than the lifetime observed in R110 ethanol/water solutions (4.04 versus 0.95 ns,³⁵ respectively). The increase of the lifetime denotes a more rigid environment of the R110 molecules, which prevents the free rearrangement of the molecules. The lack of mobility of the

TABLE 2: Maximum of Excitation (λ_{mex}) and Emission (λ_{mem}) Spectra,^{a,b} Lifetimes (τ),^c Experimental Reduced χ -Squared (χ_R^2), and Experimental Adsorption Angle (ϕ) of R110 in Gels 2–5. Data Also Included for Gel 7

	λ_{mex} (nm)	λ_{mem} (nm)	τ (ns) ^d	χ_R^2	ϕ (deg)
gel 1	503	524	4.04 ± 0.16	1.3	monomers
gel 2	504	531	4.42 ± 0.16	0.7	47.46 ± 1.12
gel 3	505	540	5.20 ± 0.18	0.6	51.44 ± 0.92
gel 4	456–506	553	6.06 ± 0.22	1.4	54.73 ± 0.77
gel 5	456–507	557	6.19 ± 0.22	1.5	55.16 ± 0.74
gel 6	456–505	561	5.74 ± 0.22	1.5	H dimers
gel 7	505	555	6.26 ± 0.14	1.3	J dimers

^a The excitation wavelength used to record the emission spectra was 410 nm. ^b The emission wavelength used to record the excitation spectra was 620 nm. ^c The excitation wavelength used to measure the lifetimes was 410 nm. ^d Errors were calculated from refs 28 and 29.

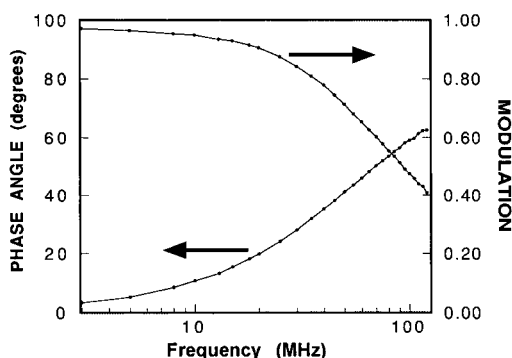


Figure 2. Lifetime results ($\lambda_{\text{ex}} = 410$ nm) for R110 doped gel 1 by the application of the PRFS method.

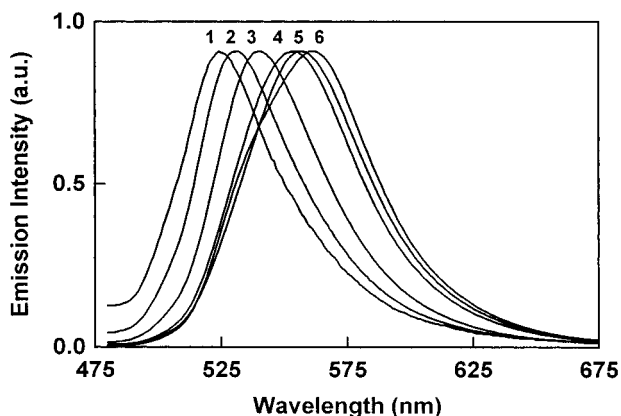


Figure 3. Emission spectra ($\lambda_{\text{ex}} = 410$ nm) of R110 doped gels 1–6.

R110 molecules in silica gel matrixes limits the intramolecular rotation modes with the subsequent reduction of the deactivation processes or quenching ($S_1 \rightarrow S_0$ internal conversion processes).^{11,13,36–38}

The increase of the R110 concentration incorporated into the silica gel-glasses (from gel 1 to gel 5, Table 1) gave rise to a progressive red shift in the emission maximum spectra of the R110-doped gel-glasses (Figure 3, Table 2). In addition, the excitation spectra recorded for gels 1–5 showed the increased intensity of a band placed at 456 nm and a shoulder resulting from the red-shift of the principal band placed at 503 nm (Figure 4, Table 2). These results are indicating the appearance of a different fluorescent species in gels 2–5 as compared to gel 1.

An additional experiment supporting the formation of this new fluorescent species was achieved. The emission spectrum of gel 5 was recorded for excitation wavelengths ranging from

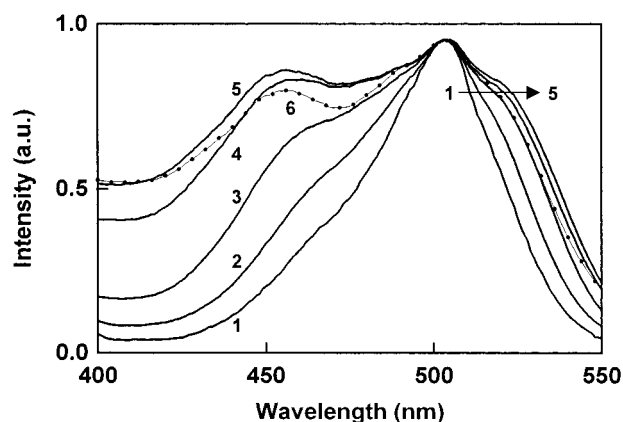


Figure 4. Excitation spectra ($\lambda_{\text{em}} = 620$ nm) of R110 doped gels 1–5 and gel 6 (●).

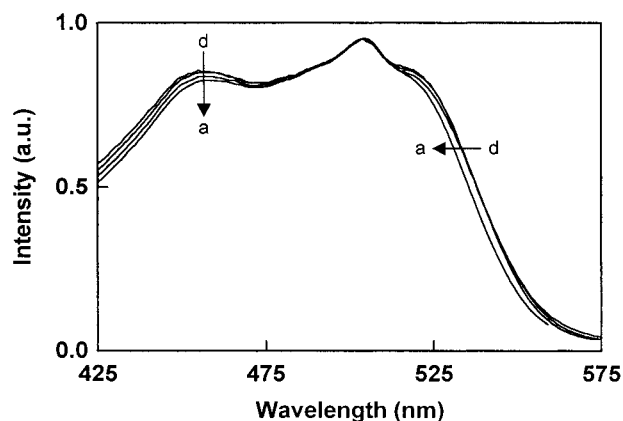


Figure 5. Excitation spectra of R110 doped gel 5 recorded at different emission wavelengths; (a) $\lambda_{\text{em}} = 580$ nm, (b) $\lambda_{\text{em}} = 600$ nm, (c) $\lambda_{\text{em}} = 620$ nm, and (d) $\lambda_{\text{em}} = 640$ nm.

TABLE 3: Modification of the Emission Maximum (λ_{em}) and the Lifetimes (τ) when Recorded at Different Excitation Wavelengths, Experimental Reduced χ -Squared Also Included

λ_{ex} (nm)	λ_{mem} (nm)	τ (ns)	χ_R^2
410	557	6.19 ± 0.22	1.1
430	556	6.12 ± 0.18	1.4
450	554	6.08 ± 0.20	1.5
480	551	5.98 ± 0.17	1.3
500	548	5.90 ± 0.15	0.8

410 to 500 nm. The emission maximum was blue shifted as far as 9 nm (Table 3). This effect can be explained based in the relative contribution of different fluorescent species to the fluorescence spectra.³⁹ Thus, in the excitation spectrum of gel 5, the main band placed around 503 nm (characteristic for monomer species) is accompanied for a new band at 456 nm (Figure 4, Table 2). Moreover, the excitation spectra recorded with different emission wavelength yielded also in the modification of the relative intensity of the excitation bands (Figure 5); i.e., the lower the emission wavelength used for recording of the excitation spectrum, the lower the relative intensity of the band at 456 nm.

Up to our knowledge, there was not spectroscopic data reported for R110-doped gel-glasses at different concentrations. A similar behavior has recently been reported for RB doped gel-glasses,¹² which is also a xanthene type molecule; i.e., in both cases, the increase of dye concentration give rise to the red shift of the main bands in the emission as well as in the excitation spectrum. The behavior of RB was attributed to the

formation of fluorescent dimers and their contribution to the fluorescence spectra.^{13,16,40} Thus, in R110-doped gel-glasses this can be a first indication of the formation of R110 fluorescent dimers.

Concerning the PRFS analysis for gels 1–5, the gradual increase of R110 lifetime values when the dye concentration increases (Table 2) is also indicating the formation of a new fluorescent species.

In concordance with the blue shift in the emission spectra observed above is the increase of the gel 5 lifetime, when the excitation wavelength increases from 410 to 500 nm (Table 3).

Since the increase of dye concentration used to yield in the formation of nonfluorescent dimers or aggregates, the above results are showing an opposite behavior to the expected; i.e., the new species formed are fluorescent rather than nonfluorescent. This unexpected behavior must be attributed to the capability of xanthenes type molecules to form fluorescent dimers at the adsorbed state.^{13,16} Formation of whether fluorescent or non-fluorescent dimers (J or H, respectively) is related to the molecular adsorption geometry on the surface. This geometry is defined by the angle (ϕ) formed between the longitudinal axis of the molecules (monomer transition moments) and the adsorption surface. Thus, formation of J-dimers has been reported for ϕ values ranging 0–55°, while over those angle values $\phi > 55^\circ$, H-dimers are formed (Figure 1).^{13,16}

According to single exciton theory,^{19,41} the radiative rate constant of the fluorescent dimers (kr_D) is related to the radiative rate constant of the monomer (kr_M) and to the geometry in which the species are adsorbed on the surface.

$$kr_D = 2kr_M \cos^2 \phi \quad (2)$$

By the calculation of kr_M from the lifetime of gel 1 (the excitation spectrum of gel 1 did not show any trace of dimers, Figure 4), and kr_D of the gels 2–5 from their respective lifetime values (gel 2–5 excitation spectra show the appearance of fluorescent dimers species, Figure 4), the experimental ϕ angle values for gels 2–5 (Table 2) can be obtained from the equation described above. The calculated ϕ angles for the adsorption of R110 molecules in gels 2–5 was lower than 55°, and accordingly these were ascribed to the presence of J-dimers in these gels. It has to be pointed out that the ϕ angle calculated for gel 5 is at the limiting value accepted for the formation of J-dimers ($\phi \approx 55^\circ$, Table 2). Thus, further increase of concentration (gel 6) would give rise to the formation of H dimers. The J to H dimer conversion was experimentally observed by the decrease of the gel 6 lifetime as compared to gel 5 (Table 2), i.e., the formation of nonfluorescent H dimers contributes to the quenching of the excited states through intersystem crossing processes.^{19,38,42–44} Moreover, compared to gel 5, the excitation spectrum of gel 6 shows a decrease of the two J-dimers characteristics bands: the band at 456 nm and the hidden shoulder at 505 nm (Figure 4).

The capability to measure an angle of adsorption depends upon having a reference surface. The determination of the surface for adsorption may be difficult since the entrapment process of the molecule within the pore matrix may give rise to a situation where the siloxane chains of the silica network goes in all directions and in all angles around the entrapped molecule. Thus, if the fluorescent molecules were totally constrained by the pores of the gel-glass, there would not be such a reference surface. However, measurements of the steady-state fluorescence anisotropy of gel 1 indicated that the fluorescent molecules are not totally constrained within the pore of the gel-glasses (0.332 for gel 1 versus 0.38–0.4 for

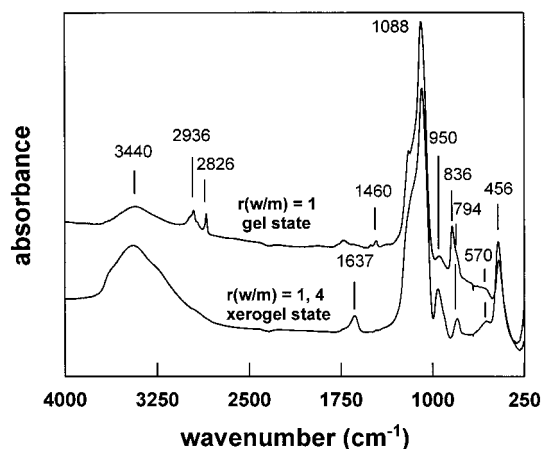


Figure 6. FT-IR spectra of gel-glasses prepared from $r_{w/m} = 4$ and $r_{w/m} = 1$ at the xerogel state. Typical bands ascribed to silica gels were observed:^{58–60} Si–O–Si asymmetric bond stretching at 1088 and 794 cm^{-1} , Si–O–Si bending at 456 cm^{-1} , SiO–H stretching at 3440, Si–OH or Si–O stretching at 950 and 560 cm^{-1} ; and H_2O molecules absorbed on the silica surface at 3440 cm^{-1} and 1620–1660 cm^{-1} . FT-IR spectra of gel-glasses prepared from $r_{w/m} = 1$ at the gel state showed bands at around 2936–2826 and 836 cm^{-1} , which are characteristic of the vibration of C–H and Si–OR bonds, respectively.^{61–63} The decrease of the intensity of the bands characteristic for Si–OH groups and H_2O molecules is also observed in the FT-IR (bands at around 3440 and 950 cm^{-1}). The typical bands characteristic of SiO_2 gels network structure can also be observed (1088, 794, and 456 cm^{-1}).

rhodamines in a vitrified system).^{9,34} This high anisotropy value corroborates that R110 is adsorbed on the porous surface, but it keeps a certain degree of mobility. Thus, it can be assumed that the fluorescent molecules are closely interacting just through one of its molecular edge with the pore surface, which is considered as the adsorption surface. The steady-state fluorescence anisotropy of gel 2 showed a slightly higher value than gel 1 (0.337 and 0.332, respectively) as corresponding to the establishment of linkage forces between the monomeric constituents of the aggregates, but still below the expected value for a vitrified system. In this case, since the aggregates are already formed at the gel state,^{40,45,46} further condensation and shrinking of the silica network is expected to occur surrounding these aggregates.^{8,12,46} The measurement of the anisotropy in gels 3–5 was not accurate because of reabsorption processes resulting from the increase of the R110 concentration.³²

The results are showing a similar behavior between R110- and RB-doped gel-glasses, both from the point of view of the adsorption on the surface as well as of the concentration value for the J to H dimer conversion.¹² This shows the minor influence that different substitutes linked to the nitrogen atom ($-\text{N}(\text{CH}_2-\text{CH}_3)_2$ for RB or $-\text{NH}_2$ for R110) have on the dye adsorption behavior. As a consequence, the dye adsorption on the porous surface should be governed by the carbonyl group.^{4,5} It has to be pointed out that the xanthene fluorescence properties are not modified by the carboxylic group ionization, as well as by the configuration adopted between the phenyl and the xanthene rings.^{11,47} This is an important point to have in account, since in this paper, the fluorescent properties of the R110-doped gel-glasses have just been related to the geometry of the adsorbed molecules.

2. Formation of Fluorescent Dimers by Reducing the Adsorption Surface Area. Since the adsorption angle is related to the available S_A , the formation of J dimers has been attempted by the preparation of gels (gels 3 and 7) with similar concentration (3×10^{-8} mol) but different S_A (36 and 390 m^2/g , respectively). This is an alternative approach to the experiments

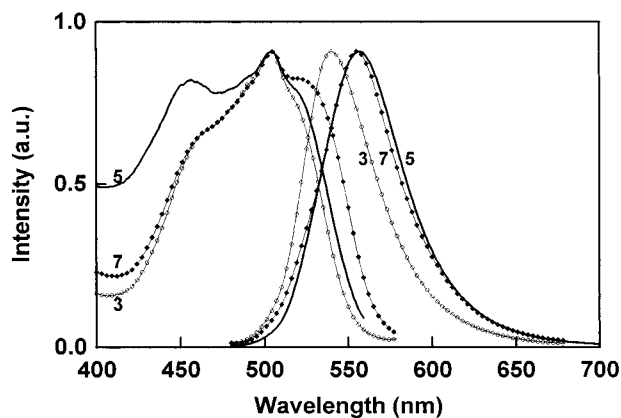


Figure 7. Excitation ($\lambda_{\text{ex}} = 410$ nm) and emission spectra ($\lambda_{\text{em}} = 620$ nm) of R110 doped gel **3** (○), gel **5** (—), and gel **7** (◆).

described above; i.e., gels **1–5** had different R110 concentrations but a similar S_A (≈ 390 m²/g).

As described in the experimental part, a gel of low S_A value was prepared by the use of understoichiometric water to monomer molar ratios at the initial stage of the sol–gel process (gel **7**, $S_A \approx 36$ m²/g). The porous surface of gel **7** is mostly composed of Si–OH groups and it is quite similar to gels prepared in stoichiometric conditions, gels **1–5** (Figure 6).²⁰ For an adequate comparison between gels prepared from different stoichiometric conditions, it is important to have similar dye-surface chemical interactions at the xerogel state.

As compared to gel **3** ($S_A \approx 390$ m²/g), the fluorescence excitation and emission maxima of gel **7** were red shifted (Figure 7). In addition, the gel **7** lifetime was larger than the gel **3** (Table 2). These results confirmed that, when the dye concentration is fixed, the decrease of the available S_A for molecular adsorption promotes not only the aggregation of the R110 monomer species but also the increase of the adsorption angle.

It has to be pointed out that the emission maximum and the lifetime value of gel **7** were similar to those found for gel **5** (Table 2). This behavior can be explained having in account that gel **5** to gel **3** concentration ratio is close (closest than for any other gel) to the gel **5** to gel **7** S_A ratio (24/3 and 390/36,

respectively). On the other hand, the gel **7** excitation spectrum did not show any band around 456 nm (Figure 7). The observation of this band in the excitation spectrum of gel **5** must be explained due to the two different configurations that R110 J-dimers can adopt on the porous surface; i.e., *oblique* and *coplanar inclined* (Figure 8). As established by exciton theory,⁴¹ dimers formation determine the appearance of two excited states (exciton splitting, Figure 8a), typically placed at lower and higher energy than the monomer excited state. On the basis of group theory, the singlet–singlet electronic transition from steady state is allowed for both excited states for *oblique* dimers, while it is only allowed for the lowest excited state for *coplanar inclined* dimers (Figure 8b). As a consequence, the appearance of two bands (red and blue shifted referred to the typical band for nonaggregates) in the excitation spectrum of gel **5** denotes the preferential formation of *oblique* J dimers. The presence of a single band (red shifted referred to the typical band for nonaggregates) in the excitation spectrum of gel **7** denotes the preferential formation of *coplanar inclined* J dimers.

The preferential formation of whether *oblique* or *coplanar inclined* dimers must be explained in terms of the chemical dye–surface interactions derived from the starting conditions of the sol-gel process. The understoichiometric water-to-monomer ratio used in the preparation of gel **7** gave rise to the presence of non-hydrolyzed groups (Si–OCH₃) on the porous surface right after gelation (Figure 6). The hydrophobic character of the non-hydrolyzed groups determines the dye-surface chemical interactions. Thus, the R110 adsorption takes place with the xanthene ring parallel to the surface in order to minimize hydrophilic interactions. The high surface coverage determined by this arrangement of the R110 molecules should give rise to the formation of *in line* dimers configuration.⁴⁸ It is known that the water diffusion from air through the open porosity of the gel causes the hydrolysis of remaining Si–OCH₃ groups and the subsequent change of the surface polarity (from hydrophobic Si–OCH₃ groups to hydrophilic Si–OH groups). Hydrolysis and condensation of remaining Si–OH groups (shrinking), and evaporation of byproducts (drying), give rise to a decrease of the S_A . All these modifications determine the transition of the R110 dimers configuration on the porous surface from *in line*

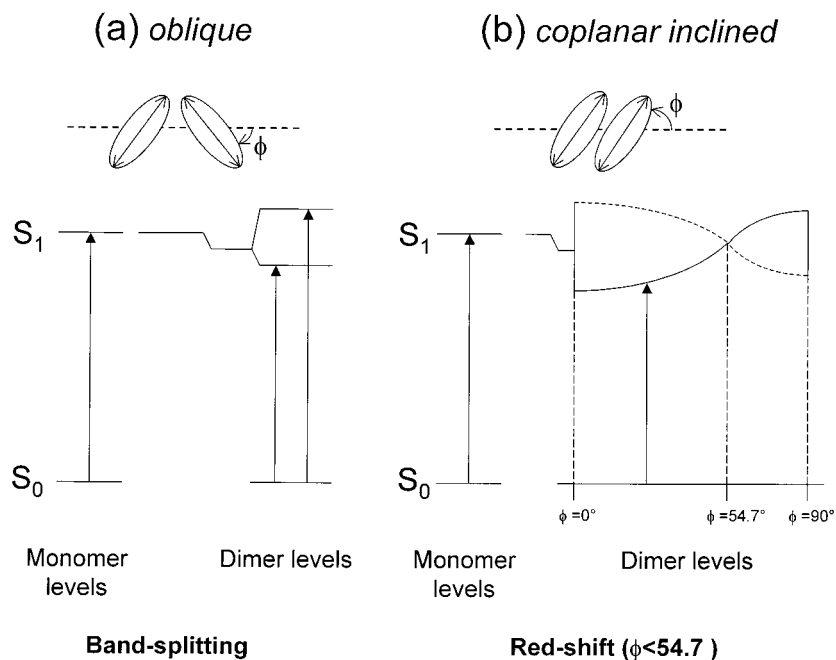


Figure 8. Exciton band energy diagram for molecular dimers with *oblique* (a) or *coplanar inclined* (b) transition dipoles, from Kasha et al.¹⁹

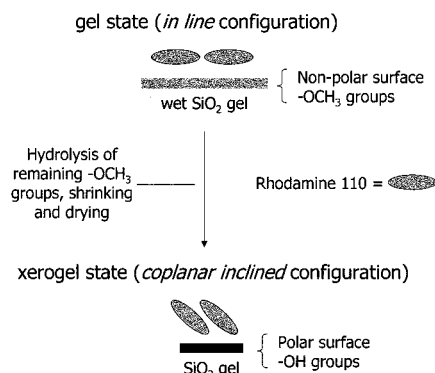


Figure 9. Schematic representation for the formation of J dimers with *coplanar inclined* configuration in gel 7.

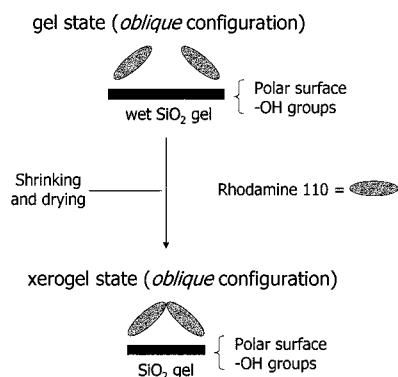


Figure 10. Schematic representation for the formation of J-dimers with *oblique* configuration in gels 1–5.

to *coplanar* (Figure 9). The preferential dimer transition from *in line* to *coplanar inclined* rather than to *oblique* configuration is established by the definition of dimers with *coplanar inclined* transition dipoles as an intermediate configuration of dimers with *in line* ($\phi = 0^\circ$ in Figure 8b) and *parallel* ($\phi = 90^\circ$ in Figure 8b) transition dipoles.^{19,41}

On the other hand, the stoichiometric water-to-monomer ratio used in the preparation of gel 5 determines the complete hydrolysis of every Si–OCH₃ groups before gelation. Thus, the hydrophilic character of the porous surface (Si–OH, Figure 10) favored the R110 adsorption in a perpendicular rather than in a parallel arrangement to the surface.

The Figures 9 and 10 represent the porous surface where dimers are adsorbed as a flat surface. It is well-known that the porous surface of gel-glasses is irregular, rather than flat. However, the irregularities of the porous surface can be considered to be minimized at small length scales ($\sim 1 \text{ nm}^2$).⁴⁹ Such a small length scale is the expected covered surface by the rhodamines according to the recently reported dimensional parameters of rhodamine aggregates.^{48,50–54} The calculation of the dimensional parameters of J-dimers doped in sol-gel-glasses through the application of the exciton theory on the excitation spectra of the fluorescent aggregates is the subject of our future work in this interesting field.⁵⁵

Conclusions

R110 fluorescent J-dimers were observed in gel-glasses as a consequence of their geometry adsorption on the porous silica surface. The identification of these species was achieved by the analysis of their photophysical properties such as excitation/fluorescence spectra and lifetimes. Moreover, the excitation spectrum denoted the preferential formation of J dimers in an *oblique* configuration. The fluorescent character of the R110

dimers was determined by the adsorption angle formed with the surface. It was found that the increase of the R110 concentration gives rise to an increase of the adsorption angle. Thus, the transition from J dimers ($\phi < 54.7^\circ$) to H dimers ($\phi > 54.7^\circ$) was found for a specific R110 concentration.

Formation of R110 fluorescent J dimers can also be achieved through an alternative approach by the decrease of the S_A available for adsorption while keeping the R110 concentration fixed. The chemical modifications introduced in the sol–gel process in order to decrease the S_A gave rise to the formation of J dimers with a *coplanar inclined* rather than with an *oblique* configuration.

It has to be pointed out the large tunability both in the emission spectrum as well as in the lifetime values observed just by the modification of the R110 concentration incorporated to the gel-glasses prepared in this study: $\lambda_{\text{mem}} \approx 524 \text{ nm} - 557 \text{ nm} = 33 \text{ nm}$, $\tau \approx 4.04 \text{ ns} - 6.19 \text{ ns} = 2.15 \text{ ns}$. This large tunability makes these systems good candidates for the preparation of R110 solid tunable laser dyes.^{56,57} No degradation processes were observed with time (more than 24 months) in normal conditions of humidity, pressure and temperature.

Finally, it is remarkable how similar is the R110 adsorption pattern observed in this paper as compared to the previously reported for RB. Therefore, it might be concluded that the geometry adsorption pattern of xanthenes type molecules is not related to the substituents linked to the nitrogen atom ($-\text{NR}_2$, $\text{R}=\text{H}$ for R110 or CH_2-CH_3 for RB).

Acknowledgment. The authors are grateful to CICYT for the research Grant ESP98-1332-C04-04 and to Carlos Alonso for technical support.

References and Notes

- (1) Brinker, C. J.; Scherer, G. W. *Sol Gel Science*; Academic Press: San Diego, 1990.
- (2) Hench, L. L.; West, J. K. *Chem. Rev.* **1990**, *90*, 33.
- (3) Ulrich, D. R. *J. Non-Cryst. Solids* **1988**, *100*, 174.
- (4) Avnir, D.; Levy, D.; Reisfeld, R. *J. Phys. Chem.* **1984**, *88*, 5956.
- (5) Avnir, D.; Kaufman, V. R. *Langmuir* **1986**, *2*, 717.
- (6) Leveau, B.; Herlet, N.; Livage, J.; Sanchez, C. *Chem. Phys. Lett.* **1993**, *206*, 15.
- (7) del Monte, F.; Levy, D. *Chem. Mater.* **1995**, *7*, 292.
- (8) Innocenzi, P.; Kozuka, H.; Yoko, T. *J. Non-Cryst. Solids* **1996**, *201*, 26.
- (9) Narang, U.; Jordan, J. D.; Bright, F. V.; Prasad, P. N. *J. Phys. Chem.* **1994**, *98*, 8101.
- (10) Lopez-Arbeloa, I.; Ruiz-Ojeda, P. *Chem. Phys. Lett.* **1981**, *79*, 347.
- (11) Drexhage, K. H. *Topics in Applied Physics*; Schäfer, F. P., Ed.; Springer: Berlin, 1973; p 144.
- (12) del Monte, F.; Levy, D. *J. Phys. Chem. B* **1998**, *102*, 8036.
- (13) Kemnitz, K.; Yoshihara, K. *J. Phys. Chem.* **1991**, *95*, 6095.
- (14) Muto, J. *J. Phys. Chem.* **1976**, *80*, 1342.
- (15) Itho, K.; Chiyokawa, Y.; Nakao, M.; Honda, K. *J. Am. Chem. Soc.* **1984**, *106*, 1620.
- (16) Kemnitz, K.; Tamai, N.; Yamazaki, I.; Nakashima, N.; Yoshihara, K. *J. Phys. Chem.* **1986**, *90*, 5094.
- (17) El Baraka, M.; Deumié, M.; Viallet, P. *J. Photochem. Photobiol A* **1991**, *62*, 195.
- (18) Deumié, M.; El Baraka, M. *J. Photochem. Photobiol A* **1993**, *74*, 255.
- (19) Kasha, M.; Rawls, H. R.; El-Bayoumi, M. A. *Pure Appl. Chem.* **1965**, *11*, 371.
- (20) del Monte, F.; Levy, D. *Opt. Mater.* **1998**, In press.
- (21) Brinker, C. J.; Scherer, G. W. *J. Non-Cryst. Solids* **1985**, *70*, 301.
- (22) Yoldas, B. E. *J. Mater. Sci.* **1986**, *21*, 1087.
- (23) Pouxviel, J. C.; Boilot, J. P.; Beloeil, J. C.; Lallemand, J. Y. *J. Non-Cryst. Solids* **1987**, *89*, 345.
- (24) Faraggi, M.; Peretz, P.; Roshental, I.; Weinraub, D. *Chem. Phys. Lett.* **1984**, *103*, 310.
- (25) Ferrer, M.; Lianos, P. *Langmuir* **1996**, *12*, 5620.
- (26) Sommedijk, N. A. J. M.; Poppe, A.; Gibson, C. A.; Wright, J. D. *J. Mater. Chem.* **1998**, *8* (3), 565.

- (27) Lackowicz, J. R.; Laczko, G.; Cherk, H.; Gratton, E.; Limkeman, M. *Biophys. J.* **1984**, *46*, 462.
- (28) Bevington, P. R. *Data Reduction and Error Analysis for the Physical Sciences*; McWraw-Hill, Inc.: New York, 1969; p 336.
- (29) Gratton, E.; Linkeman, M. *Biophys. J.* **1983**, *44*, 315.
- (30) Kowski, A. *Crit. Rev. Anal. Chem.* **1993**, *23*, 459.
- (31) Steiner, R. F. *Topics in Fluorescence Spectroscopy*; Lackowicz, J. R., Ed.; Plenum Press: New York, 1991; Vol. 2, Chapter 1.
- (32) Lackowicz, J. R. *Principles of Fluorescence Spectroscopy*; Plenum Press: New York, 1983; Chapter 5.
- (33) Levy, D.; Ocaña, M.; Serna, C. J. *Langmuir* **1994**, *10*, 2683.
- (34) Narang, U.; Wang, R.; Prasad, P. N.; Bright, F. V. *J. Phys. Chem.* **1994**, *98*, 17.
- (35) Quinn, M. S.; Al-Ajeel, M. S.; Al-Bahrani, F. *J. Lumin.* **1985**, *33*, 53.
- (36) Kemnitz, K.; Murao, T.; Yamazaki, I.; Nakashima, N.; Yoshihara, K. *Chem. Phys. Lett.* **1983**, *101*, 337.
- (37) Itho, K.; Honda, K. *Chem. Phys. Lett.* **1982**, *87*, 213.
- (38) Eyal, M.; Reisfeld, R.; Cherniyak, V.; Kaczmarek, L.; Grabwska, A. *Chem. Phys. Lett.* **1991**, *176*, 531.
- (39) Vyshkvarko, A. A.; Kiselev, V. F.; Paschenko, V. Z.; Plotnikov, G. S. *J. Lumin.* **1991**, *47*, 327.
- (40) Fujii, T.; Nishikiori, H.; Tamura, T. *Chem. Phys. Lett.* **1995**, *233*, 424.
- (41) McRae, E. G.; Kasha, M. *J. Chem. Phys.* **1961**, *11*, 38.
- (42) Ballet, P.; Van der Auweraer, M.; De Schyver, F. C.; Lemmtyinen, H.; Vuorimaa, E. *J. Phys. Chem.* **1996**, *100*, 13701.
- (43) Liang, Y.; Moy, P. F.; Poole, J. A.; Ponte Goncalves, A. M. *J. Phys. Chem.*, **1984**, *88*, 2451.
- (44) Nasr, C.; Liu, D.; Hotchandani, S.; Kramat, P. V. *J. Phys. Chem.* **1996**, *100*, 11054.
- (45) Fujii, T.; Ishii, A.; Anpo, M. *J. Photochem. Photobiol. A* **1990**, *54*, 231.
- (46) Nishikiori, H.; Fujii, T. *J. Phys. Chem.* **1997**, *101*, 3680.
- (47) Sadkowsky, P. J.; Fleming, G. R. *Chem. Phys. Lett.* **1978**, *57*, 526.
- (48) Lopez-Arbeloa, F.; Herranz-Martinez, J. M.; Lopez-Arbeloa, T.; Lopez-Arbeloa, I. *Langmuir* **1998**, *14*, 4566.
- (49) Zhuravlev, L. T. *Langmuir* **1987**, *3*, 316.
- (50) Tapia-Estébez, M. J.; Lopez-Arbeloa, F.; Lopez-Arbeloa, T.; Lopez-Arbeloa, I.; Schoonheydt, R. A. *Clay Miner.* **1994**, *29*, 105.
- (51) Tapia-Estébez, M. J.; Lopez-Arbeloa, F.; Lopez-Arbeloa, T.; Lopez-Arbeloa, I. *J. Colloid Interface Sci.* **1994**, *162*, 412.
- (52) Tapia-Estébez, M. J.; Lopez-Arbeloa, F.; Lopez-Arbeloa, T.; Lopez-Arbeloa, I. *Langmuir* **1993**, *9*, 3629.
- (53) Lopez-Arbeloa, F.; Tapia-Estébez, M. J.; Lopez-Arbeloa, T.; Lopez-Arbeloa, I. *Langmuir* **1995**, *11*, 3211.
- (54) Bojarski, P.; Matczuk, A.; Bojarski, C.; Kowski, A.; Kuklinski, B.; Zurkowska, G.; Diehl, H. *Chem. Phys.* **1996**, *210*, 485.
- (55) del Monte, F.; Levy, D. *J. Phys. Chem. B* **1999**. Submitted for publication.
- (56) Selwyn, J. E.; Steinfeld, J. I. *J. Phys. Chem.* **1972**, *76*, 762.
- (57) Rahn, M. D.; King, T. A. *Appl. Opt.* **1995**, *34*, 8260.
- (58) Almeida, R. M.; Guiton, T. A.; Pantano, G. C. *J. Non-Cryst. Solids* **1990**, *121*, 193.
- (59) Galeener, F. G. *Phys. Rev. B* **1979**, *19*, 4292.
- (60) Ocaña, M.; Fornes, V.; Serna, C. J. *J. Non-Cryst. Solids* **1989**, *107*, 187.
- (61) Abe, Y.; Namiki, T.; Tuchida, K.; Nagao, Y.; Misono, T. *J. Non-Cryst. Solids* **1992**, *147/148*, 47.
- (62) Niznansky, D.; Rehspringer, J. L. *J. Non-Cryst. Solids* **1995**, *180*, 191.
- (63) del Monte, F.; Levy, D. *J. Sol-Gel Sci. Technol.* **1997**, *8*, 585.